

# Stability of Monomer-Dimer Piles

Deniz Ertas<sup>(1)</sup>, Thomas C. Halsey<sup>(1)</sup>, Alex J. Levine<sup>(2)</sup> and Thomas G. Mason<sup>(1)</sup>

<sup>(1)</sup> *Corporate Strategic Research, ExxonMobil Research and Engineering, Route 22 East, Annandale, New Jersey 08801*

<sup>(2)</sup> *Department of Chemical Engineering, University of California, Santa Barbara, California 93106*

(October 27, 2018)

We measure how strong, localized contact adhesion between grains affects the maximum static critical angle,  $\theta_c$ , of a dry sand pile. By mixing dimer grains, each consisting of two spheres that have been rigidly bonded together, with simple spherical monomer grains, we create sandpiles that contain strong localized adhesion between a given particle and at most one of its neighbors. We find that  $\tan\theta_c$  increases from 0.45 to 1.1 and the grain packing fraction,  $\Phi$ , decreases from 0.58 to 0.52 as we increase the relative number fraction of dimer particles in the pile,  $\nu_d$ , from 0 to 1. We attribute the increase in  $\tan\theta_c(\nu_d)$  to the enhanced stability of dimers on the surface, which reduces the density of monomers that need to be accommodated in the most stable surface traps. A full characterization and geometrical stability analysis of surface traps provides a good quantitative agreement between experiment and theory over a wide range of  $\nu_d$ , without any fitting parameters.

45.70.Cc,61.43.Gt

## I. INTRODUCTION

The presence of adhesive forces between grains can greatly alter the physical behavior of sandpiles [1,2]. Although the importance of intergrain adhesion has been noted in many fields, ranging from soil science to civil engineering, the understanding of the physical principles governing the link between the macroscopic behavior of sandpiles in which adhesion is present and the microscopic attractive force distribution within the sandpile remains limited.

Some light has been shed on this subject recently through experimental and theoretical studies which have shown that small quantities of liquid added to a sandpile comprised of rough spherical grains can cause sufficient intergrain adhesion so that the angle of repose after failure [3] and also the maximum static angle of stability of the sandpile before failure [4], known as the critical angle,  $\theta_c$ , greatly increase. A continuum theory that links stress criteria for the macroscopic failure of the wet pile to the cohesion between grains, which in turn was attributed to the formation of liquid menisci with radii of curvature that were determined by the surface roughness characteristics of individual grains, has provided a satisfying quantitative explanation of the increase of  $\theta_c$  with the liquid volume fraction and air-liquid interfacial tension [5,4].

In this theory, each intergrain meniscus is assumed to exert the same average attractive force everywhere in the pile. This assumption appears to be valid for sufficiently wet sandpiles; however, when the volume of the wetting fluid is small enough this theory is incapable of explaining the data. There are two principal features of the small-fluid-volume data that are incompatible with the continuum theory [5]. The first is that the increase in  $\theta_c$  with small amounts of wetting fluid is independent of the surface tension of that fluid [4,6]. The second is that, in order to quantitatively fit the data, one must

assume that a small fraction of the wetting fluid is sequestered on the grains in such a way that it does not participate in the formation of inter-grain menisci that contribute to the adhesive stresses within the pile. It is possible that, at vanishingly small fluid coverage, the physical/chemical inhomogeneities of the grains' surface prevents the transport of the wetting fluid from one meniscus to another thereby allowing a wide distribution of inter-grain cohesive forces. To begin to understand the effect of such a broad distribution of inter-grain forces upon the macroscopic properties of the sandpile, we consider in this paper an extreme example of such a distribution in which some inter-grain contacts have an arbitrarily large cohesion while others have no cohesion at all. Consistent with the notion that the non-uniform distribution of inter-grain cohesion is primarily significant at low fluid volumes, we study a system designed so that each grain has at most one strong cohesive contract.

In order to begin to investigate how nonuniform distributions of microscopic attractive forces between grains can affect the overall macroscopic stability of sandpiles, we have measured maximum stability angles of dry sandpiles made by mixing a weight fraction  $\nu_d$  of dimer grains (two spherical grains rigidly bonded together) into spherical monomer grains. The measured  $\tan\theta_c(\nu_d)$  gradually increases over the entire range of  $0 < \nu_d < 1$ , despite a moderate drop in the total packing fraction of grains,  $\Phi$ , within the pile, due to the more inefficient packing of the dimers.

A detailed theoretical study of the failure mechanism of such piles leads us to the following key observations and conclusions, which enable us to quantitatively account for the increase in  $\tan\theta_c(\nu_d)$ :

(i) For piles consisting of perfectly rough particles (large intergrain friction), the stability of the free surface upon tilting is limited by the particles on the surface layer, which fail by rolling out of the surface traps they sit in.

(ii) For a given surface trap geometry, dimer particles typically remain stable up to larger tilt angles; thus, for a mixture of monomers and dimers, pile stability is limited by the monomers on the surface, provided that the dimer concentration is not too large.

(iii) Provided that individual grains rolling out of unstable traps do not initiate avalanches, the pile will remain stable as long as the density of *stable* surface traps is larger than the density of monomers on the surface layer.

(iv) The ratio of the density of monomers on the surface layer to the total density of surface traps is  $(1-\nu_d)/2$ .

(v) A statistical characterization of the particle-scale roughness of the surface associated with grain packing is necessary to determine  $\theta_c$  quantitatively.

The stability criteria for a pile consisting of a mixture of monomers and dimers with ideally rough surfaces can be cast as a purely geometrical problem under conditions where rolling-initiated surface failure is the primary mechanism that limits the stability of the pile. In this picture, monomers and dimers on the surface layer occupy surface traps formed by the particles underneath, each of which have a different stability criterion associated with the trap's shape and orientation with respect to the average surface normal and the downhill direction. For a pile to be stable at a given tilt angle, all the grains on the surface have to be sitting in a stable surface trap, suggesting that the least stable surface traps would control the overall stability of the pile.

For a pile consisting of monomers, there are actually twice as many surface traps as surface grains, and upon very gradually increasing the average tilt of the pile without disturbing the underlying grains, one finds that surface grains in traps that become unstable upon tilting can briefly roll down the pile's surface until they encounter an unoccupied stable surface trap which ends their descent, provided that at least half the surface traps remain stable so that all surface grains can be accommodated.

A detailed analysis in Sec. IV shows that it is much easier to trap dimers than monomers on a perfectly ordered close packed surface of spheres. This suggests that the stability of a random mixed pile of monomer and dimers is actually limited by the monomers on the surface, which accumulate in the most stable surface traps as  $\theta_c$  is approached. If one assumes that the dimers remain essentially stable, one might expect that only a fraction  $(1-\nu_d)/2$  of the surface traps remain stable when the pile is tilted to its maximum stability angle  $\theta_c(\nu_d)$ ; at this angle, there are just enough to accommodate all the monomers on the surface layer. A detailed experimental characterization of the positions of surface grains of random monomer and dimer piles in Sec. VB, combined with the computed stability criteria for monomers and dimers occupying surface traps in Sec. VA, provide a quantitative explanation of the measured increase in  $\theta_c(\nu_d)$  with no adjustable parameters up to  $\nu_d \approx 0.6$ , where the assumption of monomer failure begins to break down.

This good agreement over a wide range of  $\nu_d < 0.6$  re-

flects the subtle interplay between the distribution of orientational and size fluctuations of the surface traps, some of which are stabilizing and some destabilizing. Thus, accurate characterization of “grain-scale” roughness (as distinct from the microscopic surface roughness of the grains) is essential to achieve quantitative agreement between theory and experiment. The important role played by grain-scale roughness is also evident in the rheology of gravity-driven chute flows [7,8], where the precise nature of the bottom surface has significant influence on the resulting flow. Nevertheless, the results convincingly demonstrate that the stability of cohesionless grains with large inter-grain friction is indeed controlled by surface failure, and should otherwise be insensitive to the type of grain material.

In addition to clarifying the role of surface failure in the stability of piles by connecting macroscopic measurements of stability angle to grain-scale composition, these results for a well-characterized sandpile also provide a critical link between the attractive forces within the sandpile and the nonspherical geometry of a well-known fraction of constituent grains. In this respect, these measurements provide quantitative insight into similar measurements of the angle of repose after dynamic failure of less well-controlled piles of spheres and cylinders (e.g. peas and rice). From this perspective, dimers may be imagined as short elongated grains that have surface irregularities of the same order as the grain size. These irregularities promote the strong interlocking of adjacent grains, which inhibits the failure of the pile more than the typical contacts between smooth cylinders and ellipsoids.

The rest of the manuscript is arranged in the following way. In Sec. II, we present the experimental method for preparing the dimer and monomer grains, measuring the critical angle of stability and grain packing fraction of the pile as a function of the dimer content, and characterizing the surface configuration of monomer and dimer piles. The results of these measurements are also reported in this section. The development of the theoretical understanding of these results starts in the next section, Section III, in which the stability of a pile [of spherical grains] is posed as a geometrical problem. This section summarizes an earlier attempt to treat pile stability geometrically [9] and presents a different and more general strategy for the solution, which can be extended to include dimer grains. Using this approach, in Sec. IV, we fully solve the stability problem on a triangular close-packed surface layer for monomers and dimers. Section V presents a statistical analysis of the measured shape and orientation of traps on real surfaces of piles comprised solely of either monomers or dimers, and uses the method outlined in Sec. III to determine the corresponding solution to the stability angle. In Sec. VI, we summarize the main findings and insight gained from this study, as well as possible future directions.

## II. EXPERIMENTAL

We prepare the dimer grains by bonding glass spheres of radius  $d = 4.6 \pm 0.2$  mm and density  $\rho_g = 2.3$  g/cm<sup>3</sup> together using methyl acrylate glue. The glue in its carrier solvent completely coats the surfaces of the glass spheres and accumulates in a contact meniscus between the spheres. After less than one day of drying, a strong shear-rigid bond between the spheres is formed. The volume of the dried glue is much smaller than the volume of the spheres, so the two bonded grains have the appearance of an ideal dimer or doublet. Because the glue coats the entire surfaces of the grains and may thus alter the friction coefficient of the grains, we have likewise coated all the monomer grains with methyl acrylate so that the friction coefficient at the contact points between grains, whether monomers or dimers, is identical. The sandpiles are prepared by mixing together varying weight fractions  $\nu_d$  of dimer grains into monomers, as determined by a balance. The mixtures are placed in a clear plastic box having a square bottom that is 6.5 cm wide and a height of 5.5 cm, yielding an average number of spheres per pile of about three hundred.

To measure the critical angle, we employ a procedure that is identical to one that was used to study the critical angles of wet sandpiles [4]. We tilt the box at an angle, as shown in Fig. 1(a), and shake it back and forth about five times along the direction of the lower edge (normal to the page in the figure). This distributes the grains so that the surface of the pile is normal to the direction of gravity, as shown in Fig. 1(b). There is no noticeable size segregation of the grains introduced by the shaking. We have purposefully avoided tapping the pile in order to prevent a densification that could affect the pile's surface characteristics and stability [10]. We then place the lower edge of the box on a table and slowly tilt it so that the bottom rests flat on the table and normal to the direction of gravity. If the pile fails catastrophically, then no measurement is recorded, but if the pile remains stable after only isolated movement and resettling of a few grains, then a measurement of the static angle of the pile,  $\theta$ , is recorded, as shown in Fig. 1(c). After several trials, a rough determination of the stable angle is obtained, and thereafter the initial angles are not chosen randomly, but instead are kept close to this value. Using the results of ten trials, we average the values of the three largest angles to obtain the critical angle,  $\theta_c$ . This value of the critical angle is reproducible; the variation in the three angles used to obtain the average is about ten percent for all values of  $\nu_d$ . This procedure yields slightly larger angles than those found in typical angle of repose measurements in which the sandpile is induced to fail.

Figure 2 depicts  $\theta_c$  as a function of  $\nu_d$ . We find that it increases approximately linearly, from  $\tan \theta_c \approx 0.45$ , a well established value for a wide variety of dry spherical grains [9], to  $\tan \theta_c \approx 1.1$  for a sandpile comprised

completely of dimers.

We have also measured the average packing volume fraction of grains,  $\Phi$ , in the sandpile as a function of  $\nu_d$  by measuring the mass of water required to fill the voids in the pile as it stands in the tilted configuration shown in Fig. 1(a). Based on the relative number of grains at the surfaces compared to those within the pile, we estimate that the lowering of the local grain packing fraction due to the open or wall surfaces makes the measured  $\Phi$

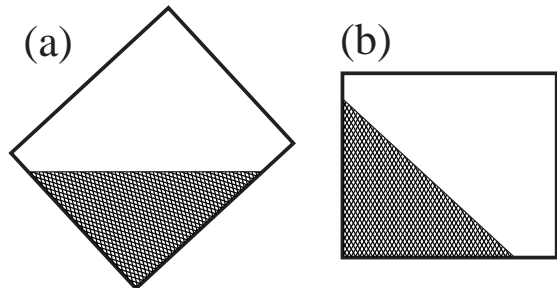


FIG. 1. Measurement of the critical angle of stability,  $\theta_c$ .

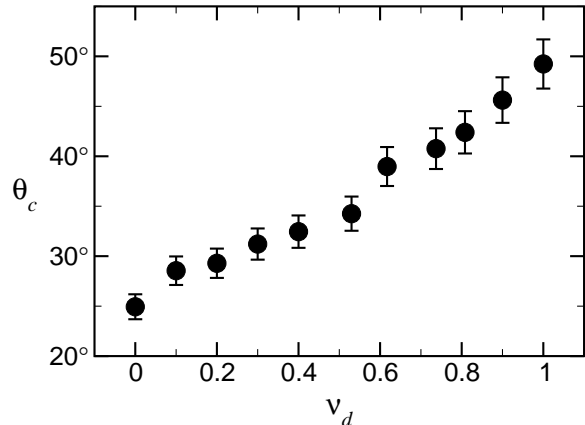


FIG. 2. The critical angle of stability,  $\theta_c$ , as a function of dimer weight fraction,  $\nu_d$ .

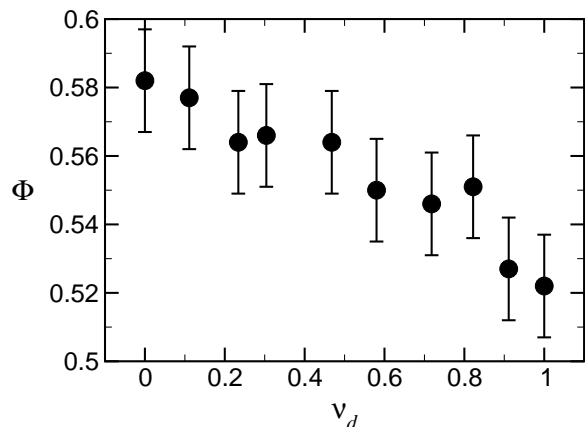


FIG. 3. The packing fraction,  $\Phi$ , as a function of dimer weight fraction,  $\nu_d$ .

appear to be about two percent smaller than the corresponding bulk value. These measurements of  $\Phi(\nu_d)$  are plotted in Fig. 3. The overall reduction in the packing fraction of about ten percent indicates that dimer grains pack less efficiently than monomer grains.

In order to experimentally characterize the surfaces of random piles of either monomer or dimer grains, we have taken stereo digital images of stable piles using top and front views in order to reconstruct the three-dimensional coordinates of the centers of all of the spheres visible on the surfaces of the piles. We do not include spheres that touch walls or the bottom surface of the container. Due to the significant surface roughness of the piles, especially in the case of the dimer pile, we occasionally detect the position of a sphere that lies more than one diameter be-

low the average surface defined by all the grains. These spheres are not true surface spheres and are eliminated from consideration in the subsequent surface trap analysis (See Sec. VB.)

The measured positions of the surface spheres for a stable monomer pile and a dimer pile are shown in Fig. 4(a) and 4(b), respectively. The monomer pile shown is very close to its critical angle of stability ( $\theta = 23^\circ$ ), whereas the dimer pile shown here, while at a much higher angle ( $\theta = 41^\circ$ ), is still somewhat below its  $\theta_c$ . Finally, we have qualitatively observed that the roughness of the sand-pile’s free surface increases somewhat as more dimers are included in the pile. This increase has been quantified in terms of larger fluctuations in the shapes and orientations of the surface traps, as presented in Sec. VB.

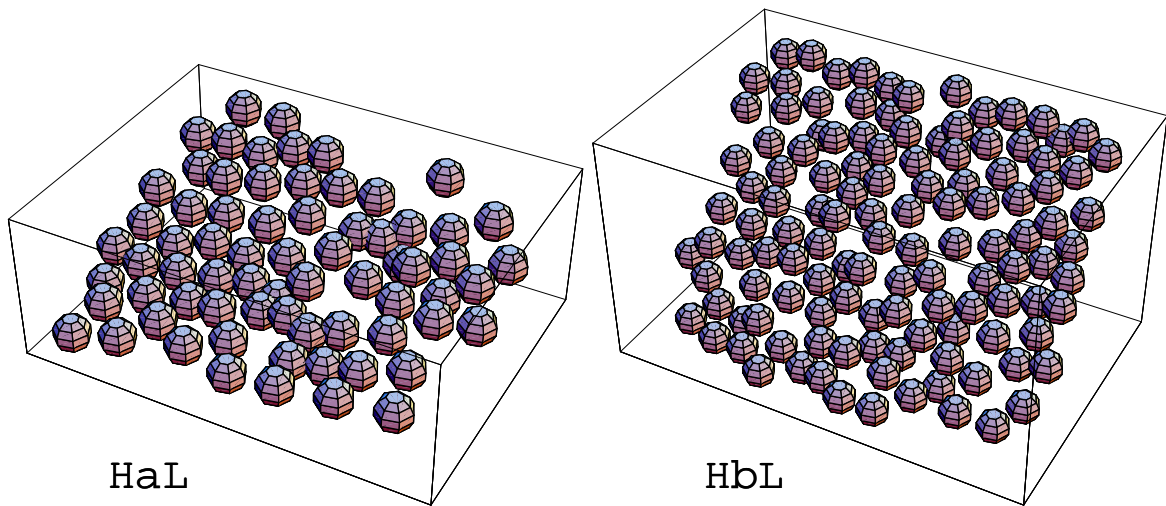


FIG. 4. Reconstructed positions of spheres at the surface of a pile consisting of (a) monomers, and (b) dimers. The technique used can identify the spheres, but not the bonds of the dimers, thus only half of a dimer might be shown in some cases. However, that information is not needed in the subsequent analysis in Sec. VB.

### III. PILE STABILITY AS A GEOMETRICAL PROBLEM

#### A. Background and Context

Various measurements of the angle of repose  $\theta_r$  for cohesionless piles of smooth spherical particles come up with the same value of about  $22^\circ$ , largely independent of the makeup of the spheres or of their surface properties [9]. On the other hand, the shape of particles in a pile has a large influence on  $\theta_r$  and the slightly larger critical angle  $\theta_c$  [11]. Furthermore, our granular dynamics simulations of piles, made of spheres with Hertzian contacts and static friction, show that  $\theta_r$  initially increases rapidly with increasing friction coefficient  $\mu$ , although it saturates at a value of about  $22^\circ$  for  $\mu > 1$  (see Fig. 5).

These observations suggest a primarily geometrical origin for the robustness of  $\theta_c$  for perfectly rough spheres ( $\mu \gg 1$ ), which can be further studied in an idealized system in which sliding is disallowed, due either to a very

large friction coefficient or to interlocking surface irregularities. The spheres in such a static pile can be classified into two groups as follows: A surface layer that consists of spheres held in place by exactly three spheres and their own weight, and interior spheres that have more than three contacts. (We do not consider the small population of “rattler” spheres with three contacts that might exist in the interior of the pile, which will presumably not influence the stability of the pile.) The centers of the three spheres that support each sphere in the surface layer form the vertices of what we henceforth call the “base triangle” associated with that sphere.

As the tilt angle of the pile is increased, spheres on the surface layer can move by rolling out of the surface trap formed by the three supporting neighbors. However, interior particles (excluding rattlers) are held in place by a cage formed by their contacting neighbors, and if the friction coefficient is sufficiently large to preclude any sliding, they cannot move until this cage is destroyed by the motion of at least one of their neighbors. This suggests that

initiation of failure occurs at the surface layer, provided that sliding is disallowed. If the coefficient for rolling friction is small enough to be neglected, the stability of a sphere on the surface layer, and consequently the determination of  $\theta_c$ , becomes a purely geometrical problem. For finite values of  $\mu$ , other failure mechanisms can be expected to reduce  $\theta_c$  from this surface controlled value, as observed in Fig. 5.

A recent attempt at a theoretical determination of  $\theta_c$  from the perspective of surface stability was made by Albert and co-workers [9]. They have considered the stability of spheres at the surface, supported by three close-packed spheres that form a base triangle, and calculated the tilt angle  $\theta_{max}$  at which the sphere would roll out of the trap formed by the base triangle as a function of “yaw”  $\phi$ , i.e., the relative angle of orientation of the triangle with respect to the downslope direction:

$$\tan \theta_{max}(\phi) = \frac{1}{2\sqrt{2} \cos(\phi)}, \quad |\phi| < \frac{\pi}{3}, \quad (1)$$

$$\theta_{max}(\phi) = \theta_{max}(\phi + 2\pi/3). \quad (2)$$

This stability criterion is periodic with period  $2\pi/3$  due to symmetry. Yaw  $\phi = 0$  corresponds to an orientation in which one of the edges of the base triangle is perpendicular to the downslope direction. In order to account for the randomness in the orientations of the base triangles on a disordered surface, they have suggested that the appropriate value for  $\theta_c$  can be obtained by averaging  $\theta_{max}$  over yaw  $\phi$ ; they assumed a uniform distribution for this quantity. This yielded a value for  $\theta_c$  that closely matched experimental observations.

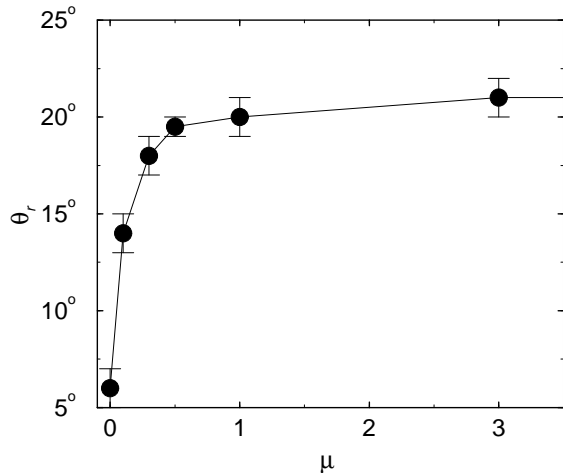


FIG. 5. Angle of repose for a pile of spheres with Hertzian contact interactions and static friction as a function of friction coefficient  $\mu$  between the spheres, obtained from granular dynamics simulations by extrapolating flow rates as a function of tilt angle to zero flow. Details of the simulation technique can be found in Refs. [7,8].

## B. Approach

As already pointed out by its authors, the calculation in Ref. [9] represents a mean-field approximation, since it ignores variations in the shape and orientation of individual surface traps, which can be parametrized by their local tilt, yaw and roll angles, and the actual edge lengths of the base triangles. (For definitions of these parameters, see the Appendix.) Nevertheless, their result is in good agreement with experiments. We will address the dependence of the stability of a surface trap on some of these additional parameters in more detail in Section V A.

There is, however, a more serious complication with the averaging approach than the neglect of fluctuation effects: The stability of the pile requires *all* particles on the surface to be stable. Thus, the stability of the pile should be dictated by the particle in the *least stable* surface trap, and not an average stability criterion. One might thus wonder why the averaging approach appears to work so well.

In fact, for a pile of monomers, the number of base triangles forming potential surface traps is essentially twice the number of surface particles that actually reside in them. This is easy to see in the case of close-packed layers, where each successive layer to be placed on top has a choice among two sublattice positions; this is what gives rise to random stacking.

The relationship is actually more general. If the surface of a pile is sufficiently smooth such that an average surface normal vector to the pile can be determined (note that this is a prerequisite to actually being able to define and measure  $\theta_c$ ), the base triangles associated with surface traps can be identified by a Delaunay triangulation of the sphere centers at the surface layer, projected onto the plane of the mean pile surface. In such a triangulation, the number of triangles per surface layer sphere is exactly two, since the sum of all the interior angles of the triangles is  $\pi \times (\text{no. triangles}) = 2\pi \times (\text{no. surface particles})$ . An intrinsic assumption here is that the surface layer is similar to the “sublayer”, consisting of those spheres that would become part of the new surface layer if all the original surface particles were removed simultaneously. The triangulation procedure to identify the surface normal vector and all of the potential surface traps is discussed in greater detail in Sec. V B.

This ratio of surface trap to surface sphere density indicates that in a stable pile, only half of the traps are actually filled. The pile will then find a stable configuration as long as at least half of the surface traps are stable at the given tilt angle of the pile, since surface spheres that are in unfavorable traps can roll down the slope until they find a vacant trap of sufficient stability, assuming that they do not gain enough kinetic energy to knock other particles off their traps and cause an avalanche. Continuous failure of surface spheres will occur if there are never enough traps to stabilize the entire layer.

This leads to the conclusion that the stability of the

pile is actually determined by the *median* stability angle of the traps, not the mean. Nevertheless, as shown in Sec. IV, the quantitative difference between this criterion and that studied in Ref. [9] is small; about 1.6 degrees.

#### IV. MONOMER-DIMER STABILITY ON A FLAT CLOSE-PACKED SURFACE

Before launching a full-scale analysis of the pile stability problem for random piles having random surface grain configurations, it is instructive to consider the implications and power of this new approach to stability on a simplified system consisting of a mixture of spheres (monomers) and dimers sitting on a triangular close-packed lattice. The stability analysis leading to Eq.(1) can be extended to dimers. Dimers sit in surface traps such that the vector connecting the centers of the two spheres forming the dimer are always parallel to one of the edges of the base triangles, thus their orientation with respect to the downhill direction can be described by the angle  $\phi$  as well. The resulting stability angle as a function of  $\phi$ , defined in the interval  $(-\pi, \pi)$ , is:

$$\tan \theta_{max}^{dimer}(\phi) = \begin{cases} \frac{1}{2\sqrt{2}\cos(\phi)}, & |\phi| < \arctan(3\sqrt{3}), \\ \frac{\sqrt{2}}{\cos(\phi-2\pi/3)}, & \arctan(3\sqrt{3}) < |\phi| < 2\pi/3, \\ \frac{1}{\sqrt{2}\cos(\phi-\pi)}, & 2\pi/3 < |\phi| < \pi. \end{cases} \quad (3)$$

The two functions defined by Eqs.(1) and (3) are plotted in Fig. 6(a). It is striking how much more stable dimers are compared to spheres for certain orientations of the traps. This is due to the more favorable position of the center of mass of the dimer, located where the two spheres meet, which makes it more difficult to roll out of the surface traps. An alternate, and perhaps more vivid, way of seeing the relative stability of dimers with respect to monomers is to plot the fraction of stable traps  $f_{stab}(\theta)$  at a given tilt angle  $\theta$ :

$$f_{stab}(\theta) \equiv \int_{\theta}^{\pi/2} d\theta' DOS(\theta'), \quad (4)$$

$$DOS(\theta) \equiv \int_{-\pi}^{\pi} d\phi \mathcal{P}_{yaw}(\phi) \delta(\theta - \theta_{max}(\phi)), \quad (5)$$

$$\mathcal{P}_{yaw}(\phi) = \frac{1}{2\pi}, \quad -\pi < \phi < \pi. \quad (6)$$

$$(7)$$

In the above,  $f_{stab}(\theta)$  is defined in terms of the density of surface traps at a given stability angle,  $DOS(\theta)$ . For this particular case, the distribution of yaw  $\mathcal{P}_{yaw}(\phi)$  is assumed to be uniform in the interval  $(-\pi, \pi)$ , corresponding to an isotropic surface geometry. The resulting plot of  $f_{stab}(\theta)$  for monomers and dimers is shown in Fig. 6(b), and clearly demonstrates the difference in their

stability. Consequently, the critical angles of stability inferred from the median stability angle for monomers and dimers are:

$$\theta_c^{monomer} = 22.2^\circ, \quad (8)$$

$$\theta_c^{dimer} = 38.3^\circ. \quad (9)$$

Values obtained through the averaging procedure of Albert *et al.* [9] are only slightly larger:  $\theta_c^{monomer} = 23.8^\circ$  [12] and  $\theta_c^{dimer} = 39.5^\circ$ .

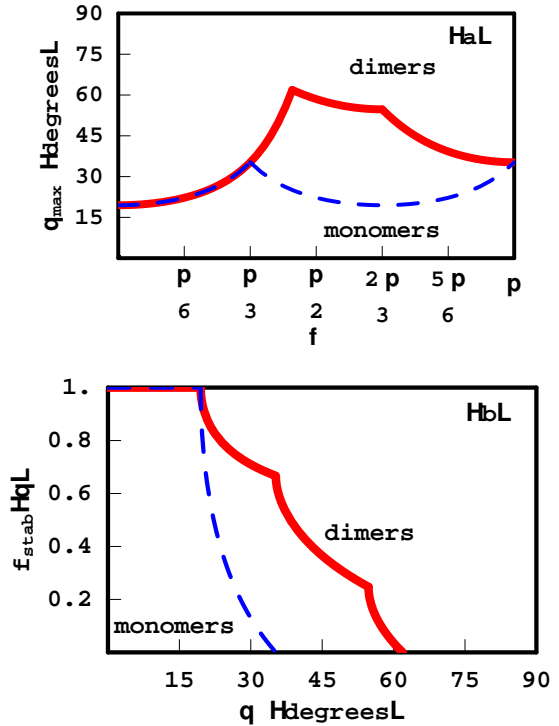


FIG. 6. (a) Stability angle of monomers (dashed line) and dimers (solid line) on a close-packed surface as a function of orientation (yaw)  $\phi$ . Monomer and dimer curves are identical for  $0 < \phi < \pi/3$ . (b) The fraction of stable traps at a given tilt angle  $\theta$  corresponding to a population of monomers (dashed line) and dimers (solid line) in surface traps with a uniform yaw distribution.

For a surface layer consisting of a mixture of spheres and dimers, with a dimer volume fraction of  $\nu_d$ , the stability of the surface layer will be primarily controlled by the monomers, since dimers will be stable at most locations on the surface at  $\theta_c$  and do not need to be considered as surface particles for the purposes of the stability analysis. Thus, for a given tilt angle, the surface layer can find a stable configuration as long as the fraction of stable traps at that angle,  $f_{stab}(\theta)$ , exceeds  $(1 - \nu_d)/2$ , the density needed to accommodate all the monomers.

The sequential filling of surface traps starting from the most stable one is somewhat analogous to the filling of an energy band in a fermionic system, with  $-\theta_{max}$  for a trap corresponding to the energy  $E$  of a fermionic state.  $DOS(\theta)$  can then be interpreted as a ‘‘Density of States’’.

The monomer pile is analogous to a half-filled energy band and the addition of dimers lowers the filling fraction from  $1/2$ . Thus, the critical stability angle  $\theta_c^{\text{mix}}(\nu_d)$  is determined by the ‘‘Fermi energy’’ of the system at the given filling fraction, defined through the implicit relation

$$f_{\text{stab}}(\theta_c^{\text{mix}}(\nu_d)) = \frac{1 - \nu_d}{2}. \quad (10)$$

This relation has been plotted as a dashed line along with experimental data for  $\theta_c$  in Fig. 7. Although it captures the essential features of the dependence on dimer mass fraction and provides a compelling mechanism for this effect, the results are not quantitatively comparable. The origin of the discrepancy lies primarily in the simplifications made in characterizing the surface: Fluctuations in the shape and orientation of surface traps will broaden the DOS spectrum and consequently change the values obtained for  $\theta_c$ . In Section V, we include the most relevant of such fluctuations in the analysis and compare results to available experimental data on the properties of such surfaces. Agreement between theory and experiment improves significantly when such fluctuation effects are taken into account.

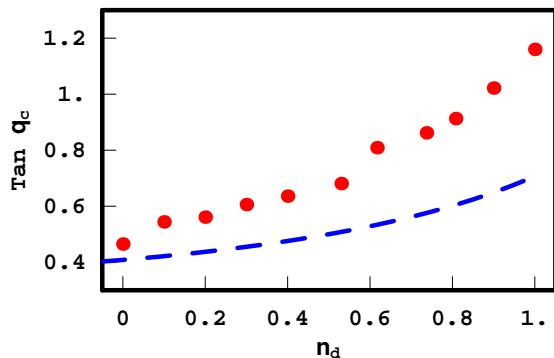


FIG. 7. Measured and calculated values of  $\theta_c$  as a function of dimer weight fraction  $\nu_d$ . Circles: Experiment. Dashed Line: Computation based on a randomly oriented, flat, close-packed surface.

## V. MONOMER STABILITY ON A RANDOM SURFACE

In generalizing the approach of the previous section to random surfaces, we will assume that the stability of the pile is still controlled entirely by the monomers. This assumption is likely to break down at very large dimer concentrations, so that comparison to experiments may not be appropriate in that case. However, it enables the determination of stability angles based entirely on the behavior of monomers, and avoids the extremely tedious analysis of dimer surface traps. Monomer traps, on the other hand, are completely characterized by their base triangle, formed by the centers of the three supporting spheres.

There are two steps that are needed to obtain the monomer DOS required to compute  $\theta_c^{\text{mix}}(\nu_d)$  through

Eq. (10). The first step is to determine the stability criterion for individual surface traps as a function of their shape and orientation. The second step is to develop an adequate statistical description of the distributions of these surface traps as functions of the shape and orientation parameters identified in the first step.

### A. Stability of a surface trap

For a surface trap of specified geometry, represented by its base triangle, what is the angle to which the pile can be tilted until the trap can no longer stably support a sphere and the sphere would roll out? In order to answer this question, we first need to quantitatively describe the geometry of the surface trap with respect to the surface of the pile. This is done in the Appendix, where the yaw  $\phi$ , roll  $\psi$  and tilt  $\theta$  of a base triangle are defined (See Fig. 12.)

The determination of stability criteria as a function of shape, yaw and roll is a straightforward but tedious job. We have used a Mathematica notebook to compute the stability diagram for equilateral traps as a function of normalized average edge length  $a \equiv (l_1 + l_2 + l_3)/(3d)$ , yaw  $\phi$ , and roll  $\psi$ , where  $d$  is the diameter of the spheres.

The dependence of the maximum stability angle  $\theta_{\text{max}}$  on  $a$  for traps with  $\psi = 0$  is plotted in Fig. 8a. It is clear that this parameter greatly influences the stability of the pile. In order to estimate the value of  $a$  for a random packing of spheres with a given packing fraction  $\Phi$ , let us consider the tetrahedra in a Delaunay tessellation of the packing. Provided that the number of tetrahedra per sphere do not change for the packings of interest, the average volume of the tetrahedra will vary as  $V_{\text{tet}} \sim \Phi^{-1}$ . Spheres on the surface layer will settle into the minima of their traps, thus the tetrahedra they form together with their three supporting spheres always have three edges whose lengths are equal to the diameter  $d$ . Thus, the average edge length of the faces that form the base triangle is expected to vary as  $l_{\text{av}} \sim \Phi^{-1/2}$ . Since all edge lengths are equal to  $d$  for the densest packing with  $\Phi_{\text{cp}} = 0.74$ , the estimate for the average normalized edge length of base triangles is

$$a(\Phi) \approx \left( \frac{\Phi}{0.74} \right)^{-1/2}. \quad (11)$$

For the monomer pile with  $\Phi = 0.58$ , this gives  $a = 1.13$ , in agreement with direct measurements done on the pile (see Sec. VB.)

Fig. 8b shows  $\theta_{\text{max}}$  against  $\phi$  and  $\psi$  for surface traps with  $a = 1.13$ . (For certain values of yaw and roll, there is no tilt angle for which the traps are stable, and therefore  $\theta_{\text{max}}$  is undefined.)

The analysis in Ref. [9] is more limited in the types of surface traps it considers, as it only looks at traps with  $a = 1$  and  $\phi = 0$ . As seen in Fig. 9, roll and edge length

have great potential impact on the stability of a surface trap. Although the Mathematica notebook can determine the stability diagram for the most general case, we will restrict our analysis to equilateral traps in order to keep the subsequent analysis tractable.

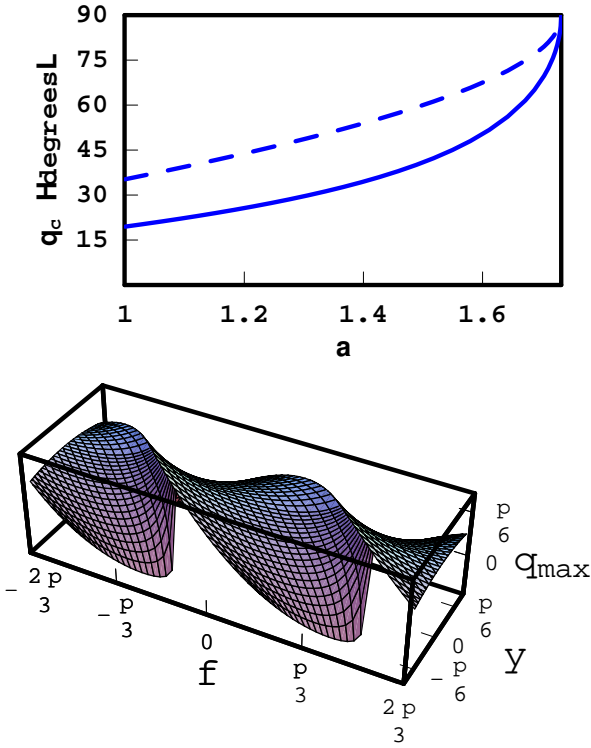


FIG. 8. The maximum stability angle  $\theta_{max}$  of equilateral traps as a function of (a) normalized edge length  $a$  for roll  $\psi = 0$ , and yaw  $\phi = 0$  (solid line) and  $\phi = 30^\circ$  (dashed line); (b)  $\theta_{max}$  as a function of yaw  $\phi$  and roll  $\psi$  for  $a = 1.13$ .

## B. Statistical description of traps on the surface of a pile

Having characterized and obtained stability criteria for a given surface trap, the next task is to obtain a statistical description of their population, through probability density functions (PDFs). In this study, we will neglect short-range correlations between adjacent traps, e.g., associated with the sharing of edges, and assume that they are drawn independently from an ensemble described by PDFs for the values of edge lengths, yaw, roll, and tilt. For the present, we will assume that all traps are equilateral triangles with edge length  $ad$ , with uniformly distributed yaw angles and Gaussian roll and tilt angle distributions:

$$\mathcal{P}_{\text{shape}}(l_1, l_2, l_3) = \delta(l_1 - ad)\delta(l_2 - ad)\delta(l_3 - ad), \quad (12)$$

$$\mathcal{P}_{\text{yaw}}(\phi) = \frac{1}{2\pi}, \quad -\pi < \phi < \pi, \quad (13)$$

$$\mathcal{P}_{\text{roll}}(\psi) = \frac{1}{2\pi\sigma_\psi^2} e^{-\frac{\psi^2}{2\sigma_\psi^2}}, \quad (14)$$

$$\mathcal{P}_{\text{tilt}}(\theta) = \frac{1}{2\pi\sigma_\theta^2} e^{-\frac{(\theta - \theta_{\text{pile}})^2}{2\sigma_\theta^2}}. \quad (15)$$

In the above,  $\{l_i\}$  correspond to the edge lengths; we will neglect the variability in the shapes of the traps and focus on equilateral traps of uniform size in order to study the effect of orientational disorder. If desired, the subsequent analysis can be generalized to study the impact of disorder in the shapes of the traps as well.

The orientational PDFs are motivated by assuming that the pile surface was created with no initial tilt, and rotationally isotropic in the plane of the surface, and that little or no rearrangement took place in the surface traps during the subsequent tilting of the pile. This would result in a uniform PDF of yaw, and nearly identical PDFs for roll and tilt ( $\sigma_\psi \approx \sigma_\theta$ ) [13].

Fig. 9 depicts how  $\theta_c$  for a monomer pile changes as a function of change in (a) the trap size parameter  $a$ , and (b) the standard deviations of roll and tilt distributions, both individually and jointly. From these plots, it becomes clear that we need additional information about the grain-scale roughness of the surface in order to quantitatively predict  $\theta_c$  for the monomer-dimer piles.

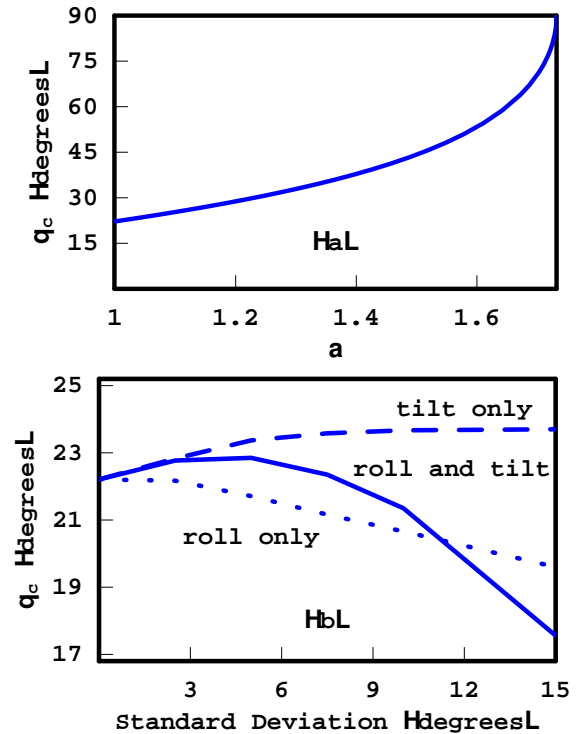


FIG. 9. The dependence of  $\theta_c$  for a monomer pile as surface properties are changed from a randomly oriented, flat, close-packed surface with no roll. (a) An increase in the normalized edge length  $a$  for equilateral traps stabilizes the traps and increases  $\theta_c$ . (b) Individual effects of including a Gaussian roll distribution (dotted line, destabilizing), tilt distribution (dashed line, stabilizing) and the combined effect of a simultaneous roll and tilt distribution with the same standard deviation (solid line, either stabilizing or destabilizing).



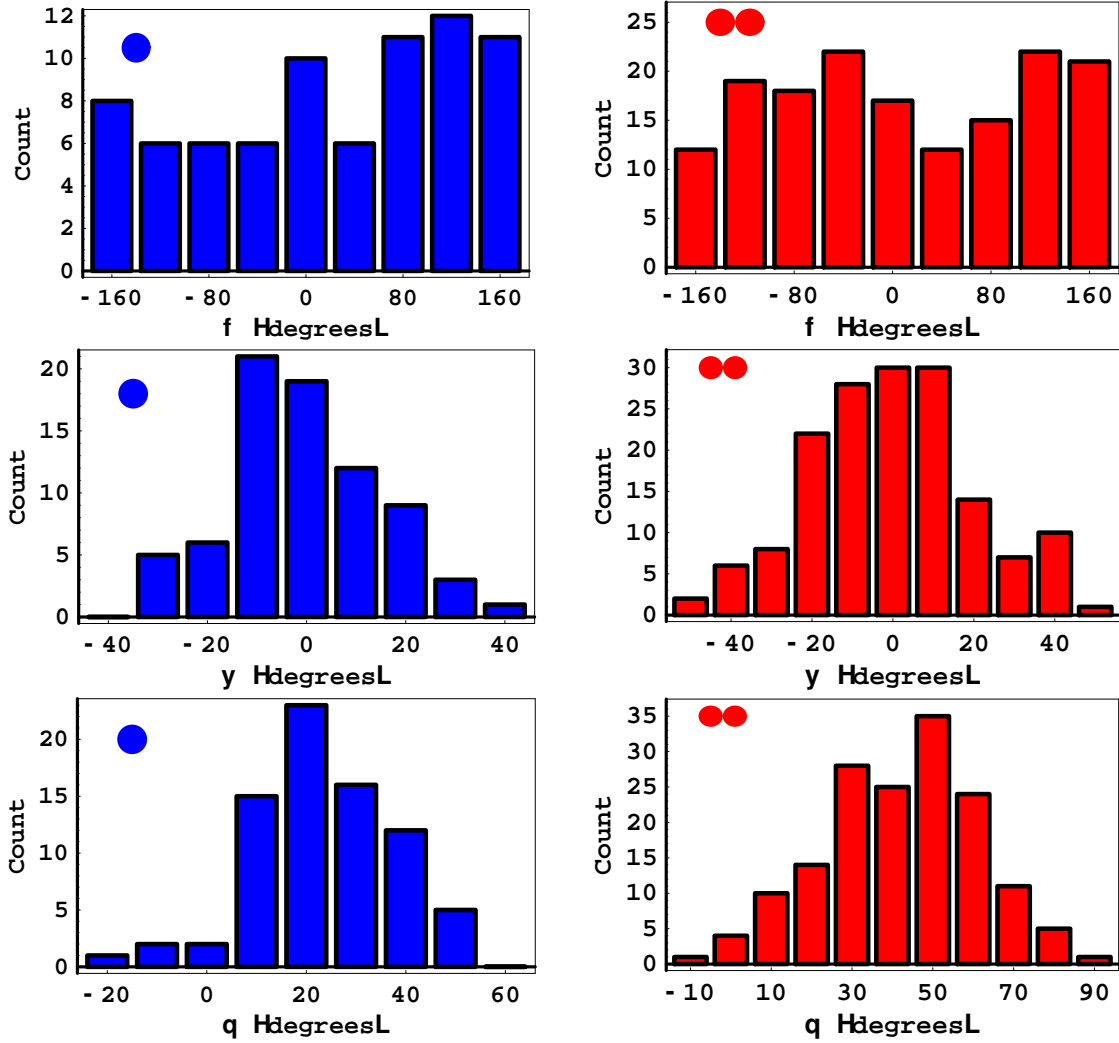


FIG. 10. Histograms of yaw, roll and tilt distributions for the piles shown in Fig. 4. *Left*: monomer pile, *Right*: dimer pile.

In order to test whether real surfaces of piles exhibit the assumed behavior, and to obtain representative values for the average trap size and the width of yaw, roll and tilt distributions, we imaged a portion of the surface of a monomer and a dimer pile (see Sec. II). The shape and orientation of surface traps were identified as follows: After locating the centers of the particles on the surface layer by stereographic imaging, we computed the average surface of the plane by a least square fitting of the centers of mass to a plane. We then performed a Delaunay triangulation of the particles projected on to this plane in order to identify all base triangles associated with potential surface traps. We then measured the yaw, roll and tilt of all the base triangles and created histograms. We observed a uniform yaw distribution within a characteristic sampling error, justifying the use of Eq.(13). We also determined the standard deviations  $\{\sigma_\psi, \sigma_\theta\}$  for the roll and tilt histograms. The histograms are shown in Figs. 10 for the monomer and dimer pile.

The comparison between the monomer and dimer piles revealed a moderate increase of  $\sigma_\psi$  and  $\sigma_\theta$  from about

$15^\circ$  to  $20^\circ$ , indicating a roughening of the surface along with the originally observed reduction in packing fraction. The average edge length increased from 1.13 to 1.18, in agreement with Eq. (11). Due to the modest changes in these parameters, we have used the trap characteristics obtained from the monomer pile in the computation of  $\theta_c$  for all the mixture piles. Integrating the stability diagram shown in Fig. 8b with the PDFs given in Eqs.(12-15) to obtain the appropriate  $DOS(\theta)$  through a generalized form of Eq.(5), we finally compute  $\theta_c^{\text{mix}}(\nu_d)$  through Eq.(4). The result is shown in Fig. 11 as a solid line, and agrees well with experiment for  $0 < \nu_d < 0.6$ , particularly considering that all the parameters have been provided by independent measurement. No adjustable parameters remain in the model, suggesting that the assumption of monomer failure at the surface is valid in this range. The disagreement at larger  $\nu_d$  is not surprising, given that the pile is comprised almost entirely of dimers and the assumption of monomer failure in the theory is expected to break down in this limit, resulting in an over-estimate of the stability of the pile.

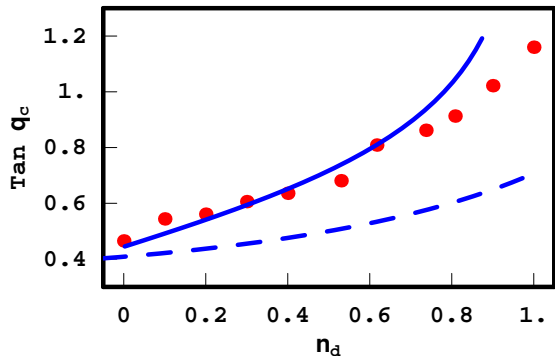


FIG. 11. Measured and calculated values of  $\tan \theta_c$  as a function of dimer weight fraction  $\nu_d$ . Circles: Experiment. Solid Line: Computation based on the statistical description of surface traps given by Eqs.(12)-(15). Dashed Line: Comparison to the earlier result based on a randomly oriented, flat, close-packed surface, reproduced from Fig. 7.

## VI. CONCLUSION

By introducing dimer grains in a sandpile comprised of rough spherical monomer grains, we have shown that the critical angle of the sandpile can be nearly doubled in the limit of high dimer content. Qualitatively, this result is not so surprising, given the significant number of previous measurements of the angle of repose of mixtures of cylindrical or spheri-cylindrical grains with spherical grains that have also shown an increase. However, the use of dimers, rather than other elongated objects, permits the random surface of the pile to be described as a collection of spheres that form triangular surface traps. These triangles have a distribution of edge lengths and yaw, roll, and tilt angles that can be directly obtained through stereo imaging and can be included in a theory. By comparing the macroscopic average property of the pile, the critical angle, with the grain-scale structure on the pile’s surface obtained through imaging, we are able to show which aspects of the surface structure are important for determining the value of the critical angle.

For instance, the treatment of the critical angle of a random pile that considers only the mean angle of stability for a grain on a close packed surface, averaged over the yaw angle, may give a value close to the measured  $\theta_c$ , but is this just a fortuitous agreement? Our results show that, by averaging over realistic distributions of yaw and tilt, the more realistic median critical angle drops below the observed  $\theta_c$ . However, because the pile is random, the intergrain separation has a distribution itself, and the average edge length of a triangular surface trap is slightly greater than the grain diameter. This increase in the edge length of the surface trap, as compared to a perfectly close packed surface, increases the stability of a sphere in the trap. Indeed, we believe that it is the combination of the destabilizing influence of the roll distribution, along with the stabilizing influence of the larger edge length that gives the random pile of rough spherical

grains its rather well-established value of  $\theta_c \approx 23^\circ$ .

These results for mixed monomer-dimer sandpiles shed some light on the observed initial increase in the critical angle of wet sandpiles, independent of container size and liquid surface tension, when liquid content is below a threshold value. [4,6]. The initial linear increase in  $\tan \theta_c$  with  $\nu_d$  may provide a plausible mechanism, in which the fraction of strongly wetted intergrain contacts increases gradually until all intergrain contacts are nearly uniformly wetted. Provided that the formed bonds are strong enough and relatively dilute, the wet pile can be expected to respond similarly to a pile with a small fraction of dimers. One would expect that clusters with grains having more than one cohesive contact with neighboring grains would form in the wet sandpile as the threshold volume fraction is approached, and, above the threshold volume fraction, the picture of an average cohesive force holding grains together everywhere in the pile would become tenable. The data in Refs. [4] and [6] suggest an equivalent  $\nu_d$  of about 0.12 at the threshold liquid volume fraction.

It may be possible to extend the presented work to systems involving trimers and higher order clusters of grains [14]. However, such clusters can have many different shapes, and to simplify the theoretical treatment, it may be necessary to restrict allowed shapes to close-packed or linear structures. Along a different direction, reducing the grain-grain friction coefficient  $\mu$  will allow sliding failure modes and thereby lower the critical angle of the sandpile. Densification of the pile through tapping might also change the angles of stability. Finally, developing a theoretical understanding of the reduction of the grain packing fraction with increasing dimer content would help shed light on how strong intergrain attractive forces can alter the bulk structure of a random pile.

We thank P. Chaikin, Z. Cheng, G. Grest and P. Schiffer for stimulating discussions and suggestions. AJL was supported in part by the National Science Foundation under Award DMR-9870785.

## APPENDIX: PARAMETERIZATION OF A SURFACE TRAP - YAW, ROLL AND TILT

In this Appendix, we define the parameters that describe the shape and orientation of a base triangle that connects the centers of mass of the three supporting spheres that form a surface trap.

The geometry is shown in Fig. 12. The coordinate system is fixed such that gravity is in the  $-z$  direction, and the pile, whose mean surface is initially in the  $xy$ -plane, is “tilted” by rotating it around the  $x$ -axis. Since overall translation of the triangle has no effect on trap stability, the vertex across the shortest edge (with length  $l_1$ ) has been arbitrarily placed on the  $z$ -axis for ease of illustration. The base triangle can be fully specified by the positions of the two remaining vertices relative to the first one; this leaves six parameters to be determined.

A more useful parameterization than the relative positions of the vertices can be given as follows (See Fig.12): The shape of the base triangle is characterized by the lengths of its edges. The two remaining edge lengths can be unambiguously labeled as  $l_2$  and  $l_3$  anticlockwise around the triangle when observed from a viewpoint above (at large  $z$ ). This leaves three angles that determine the orientation. The plane in which the base triangle resides is described by *roll*  $\psi$  and *tilt*  $\theta$ . Similarly, the orientation of the triangle in the plane with respect to the downhill direction is described by the *yaw*  $\phi$ , as depicted in Fig. 12 [15].

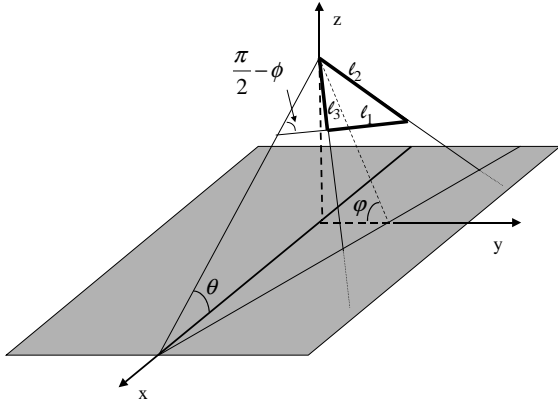


FIG. 12. The geometry of a surface trap, characterized by its yaw  $\phi$ , roll  $\psi$  and tilt  $\theta$ , as well as the edge lengths  $\{l_i\}$  of its base triangle.

Given these parameters, the original base triangle can be reconstructed (modulo translations) as follows: Place a triangle with given edge lengths in the  $xy$ -plane such that the shortest edge is parallel to the  $x$ -axis and “downhill” from the vertex across it, i.e., the  $y$ -ordinate of the vertex is larger. Then, rotate the triangle around the  $z$ -axis by  $\phi$ ,  $y$ -axis by  $\psi$  and finally,  $x$ -axis by  $\theta$ . With the proper labeling of vertices as described above, every triangle is uniquely identified except for degenerate cases (isosceles and equilateral triangles), in which case the stability criteria are identical and the particular choice of angles is immaterial.

This parameterization has two main advantages, both of which facilitate statistical averaging over many traps, performed in Sec. VB:

(i) The shapes and orientations of surface traps are very likely to be statistically independent of each other,

and therefore they will have independent probability distributions. Splitting the parameters that describe these two attributes avoids dealing with joint probability distributions across these two classes of parameters.

(ii) Tilting the pile does not change the yaw and roll of a surface trap. Thus, a “stability interval”  $[\theta_{min}, \theta_{max}]$  can be defined for a surface trap of given yaw and roll, corresponding to all the values of tilt  $\theta$  for which the trap can stably support a surface particle.

- 
- [1] R. L. Brown and J. C. Richards, *Principles of Powder Mechanics*, Pergamon Press (Oxford, 1970)
  - [2] A. Schofield and P. Wroth, *Critical State Soil Mechanics*, McGraw-Hill (Maidenhead, 1968).
  - [3] D. J. Hornbaker, R. Albert, I. Albert, A.-L. Barabási, and P. Schiffer, *Nature (London)* **387**, 765 (1997).
  - [4] T. G. Mason, A. J. Levine, D. Ertas, and T. C. Halsey, *Phys. Rev. E* **60**, R5044 (1999).
  - [5] T. C. Halsey and A. J. Levine, *Phys. Rev. Lett.* **80**, 3141 (1998).
  - [6] P. Tegzes, R. Albert, M. Paskvan, A.-L. Barabási, T. Vicsek and P. Schiffer, *Phys. Rev. E* **60**, 5823 (1999).
  - [7] D. Ertas, G. S. Grest, T. C. Halsey, D. Levine, and L. E. Silbert, cond-mat/0005051, *Europhys. Lett.* (in press).
  - [8] L. E. Silbert, D. Ertas, G. S. Grest, T. C. Halsey, and D. Levine, cond-mat/0105071, *Phys. Rev. E.* (in press).
  - [9] R. Albert, I. Albert, D. Hornbaker, P. Schiffer and A.-L. Barabási, *Phys. Rev. E* **56**, R6271 (1997).
  - [10] J. B. Knight, C. G. Fandrich, N. L. Chun, H. M. Jaeger, S. R. Nagel, *Phys. Rev. E* **51**, 3957 (1995).
  - [11] V. Frette, K. Christensen, A. Malthé-Sørensen, J. Feder, T. Jøssang and P. Meakin, *Nature* **379**, 49 (1996).
  - [12] This value was erroneously reported in Ref. [9] as 23.4°.
  - [13] The distributions of roll and tilt would not be identical since the two finite rotations do not commute. However, the difference is only third order in the angle and quite small for reasonably narrow distributions.
  - [14] C. J. Olson, C. Reichhardt, M. McCloskey and R. J. Zieve, cond-mat/0011508 (unpublished).
  - [15] We have borrowed aviation/navigation terminology to name the three angles, roll, yaw and tilt, that describe the orientation of the base triangle.